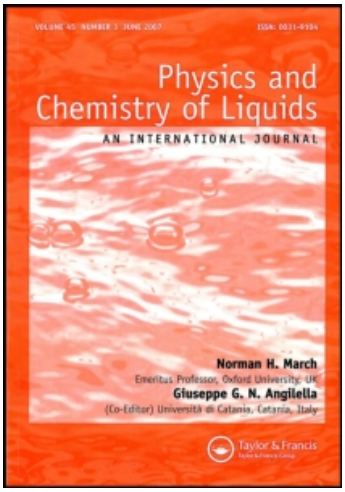

Physics and Chemistry of Liquids
Publication details, including instructions for authors and subscription information:
http://www.informaworld.com/smpp/title~content=t713646857

Dynamics of the Double Layer at the Polorizable Mercury-Electrolyte Interface

S. S. Bamji[a]; S. P. Bowen[a]; R. F. Tipsword[a]
[a] Department of Physics, Virginia Polytechnic Institute and State University, Blacksburg, Virginia

To cite this Article Bamji, S. S. , Bowen, S. P. and Tipsword, R. F.(1978) 'Dynamics of the Double Layer at the Polorizable Mercury-Electrolyte Interface', Physics and Chemistry of Liquids, 8: 3, 189 — 208
To link to this Article: DOI: 10.1080/00319107808084752
URL: http://dx.doi.org/10.1080/00319107808084752

Phys. Chem. Liq., 1978, Vol. 8, pp. 189–208

Printed in Holland

Dynamics of the Double Layer at the Polorizable Mercury-Electrolyte Interface

S. S. BAMJI,† S. P. BOWEN, and R. F. TIPSWORD

Department of Physics, Virginia Polytechnic Institute and State University, Blacksburg, Virginia 24061

(*Received March 31, 1978*).

The electric potential differences which arise across the length of capillary tubes containing 1N Perchloric acid and mercury drops are studied experimentally and theoretically for conditions of constant acceleration and constant velocity of the mercury drops relative to the capillary walls. A relatively simple theory explains many features of the dependence of the potential difference on experimental parameters. The results suggest that by coupling mechanical measurements with electrochemical measurements could yield interfacial parameters which are difficult to determine by electro chemistry alone.

I INTRODUCTION

The investigations of electrical phenomena associated with dipole layers date back to early experiments in the nineteen hundreds on streaming potentials and electrocapillarity. Due to the complexity of the electric double layers at the interfaces, there still seems to be some confusion regarding the exact mechanisms involved in producing the voltages and currents that are observed.

The book by Levich[1] provides a very comprehensive review of the subject along with an excellent bibliography. In particular, Levich[1] deals very extensively with the problem of convective flow on the dissolution of metals in electrolytes. This has some bearing on the subject we have investigated since the double layers we have studied are formed by a diffusion limited dissolution process. Our experiments were conducted on the dipole layer formed at a

† Present address: Physics Dept. Collége Militaire Royal, St. Jean, Quebec, Canada.

mercury-electrolyte (perchloric acid) interface. The diffusion limited dissolution process, in this case, means that the dipole density in the double layer is determined by a quasa-static process. In the absence of convection diffusion; the mercury droplets should be stable against significant dissolution for several months.[2] This was indeed the case for the mercury droplets in our investigation.

During the study of surface electrical phenomena, Ueda *et al.* discovered a phenomena which they called the U-effect.[3,4] In these papers, the U-effect is classified as two separate effects: U-effect I and U-effect II. The first, U-effect I, is produced by the relative motion of an electrolyte in a glass capillary with respect to the capillary walls through which electrodes have been inserted (streaming potential). The U-effect II was produced by a rapid periodic vibration of a glass capillary in which alternate drops of mercury and electrolyte (1N HCl), forming about forty interfaces, had been sealed with electrodes in the end drops of the mercury. The voltage was thought to be caused by the distortion of the double layer between the mercury-electrolyte interface when the capillary was accelerated. The double layer was considered to be similar to a condenser with the distortion of the interface changing its area, while the charge remained constant.

A further experimental and theoretical investigation of the U-effect II was made by Fain *et al.*[5] The theoretical treatment by Fain *et al.*[5] was based upon the area changes of the interfaces being treated as capacitors much as was the treatment by Ueda *et al.*[3,4]

A new effect, called U-effect III, was reported by Podolsky *et al.*[6] and was thought to be caused by the relative motion between the mercury drops and the capillary wall. They constructed a theory in agreement with their results that showed an ouput voltage independent of the number of interfaces. This result was in disagreement with Ueda *et al.*,[3,4] who found the output voltage to be a linear function of interfaces,

According to Ueda *et al.*[4] and Fain *et al.*[5] the output voltage is due to the changes in the area of the mercury electrolyte interfaces. On the other hand, Podolsky *et al.*[6] claims that the differences in the charge density at the ends of the mercury slugs, induced by the movement with respect to the capillary surface, play a decisive role especially at low frequencies. They describe two processes for the double layer to return to equilibrium after a disturbance: (1) mercurous ions are transferred across the interface at some rate constant κ; (2) dipoles diffuse over the drop from one surface to the other with some characteristic diffusion rate λ.

It has been found[5,6] that the longer the mercury drop the greater the output voltage, for short enough drops. This would tend to indicate that the dipole diffusion over the drop is of some importance. If the rate of diffusion is approximately the same order of magnitude as the transfer rate of mercurous ions

across the interface, then making the drop longer would increase the effective number of excess dipoles at one end relative to the other, thus producing a greater output voltage. Also, according to Podolsky *et al.*[6], the output voltage depends on the amount of mercury but is independent of the number of interfaces, and this contradicts the findings of Ueda *et al.*[4] and Fain *et al.*[5]. They[6] also found that the U-effect III gave rise to a potential of opposite polarity to the U-effect II.

It should be noted that the potentials observed in this experiment are not directly related to the usual phenomena of sedimentation potentials, as discussed by Levich,[1] since the mercury drops are in contact with the capillary walls and do not allow for streaming of ions in the electrolyte around the moving mercury drop. The explanation of the effects presented here is dependent on the surface tension effects and the viscous forces in the capillary tube. Similar effects, but for much larger Reynolds' numbers, have been observed by Christiansen[7] and are discussed by Levich.[1] However; the particular process involved in the current work were not considered by either Levich[1] or Christiansen.[7]

II EXPERIMENTAL TECHNIQUE

An apparatus was designed to give the mercury-electrolyte interface a constant acceleration and measurable displacement in one direction before bringing it to an abrupt stop. This is in contrast to oscillating the mercury-electrolyte interface as was done in previous investigations.

Pyrex glass capillary tubes were obtained with precision bore and had their internal diameters varying from 0.5 to 1.5 mm. At both ends of the tube, pyrex glass cups of 0.7 cm internal diameter were attached which gave the tube a dumb-bell shape with open ends as shown in Figure 1. The tubes were cleaned by drawing boiling nitric acid through them, then rinsed with equilibrium water[8] and dried in a vacuum. The electrolyte used throughout the experiment was 1N perchloric acid and the mercury was triple distilled. The tubes were filled with a single mercury drop and electrolyte on either side with teflon pistons in the glass cups to complete the capillary tube. Also, care was taken to prevent any air from entering the system. Platinum electrodes (gauge 22), across which the voltage was measured, were sealed into the tubes as shown in Figure 1.

The design of the apparatus used for accelerating the mercury drops in the capillary tubes is shown in Figure 2. The tube was fastened to the base of clamps A and the piston rods were attached to the carriage C. The carriage

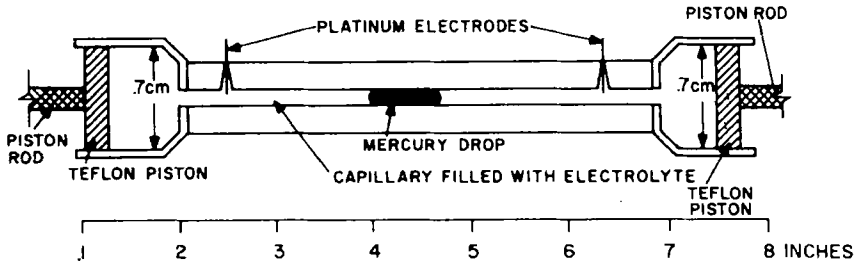

FIGURE 1 Glass capillary tube in shape of dumb-bell.

was driven against an air pressure of about 70 lbs/sq. in. by the rotation of a screw. The screw in turn was rotated by dropping a hammer with a mass attached to it from different heights onto a sponge. This caused the pistons to move in such a way that when one piston moved to the right, the other piston moved to the right also, so that the mercury-electrolyte system was given an acceleration and net displacement to the right. By releasing the hammer from different heights and with different masses attached to it, the mercury drop could be accelerated at different rates (since the internal friction remained constant) and achieve different maximum velocities. The net displacement of the mercury drop was read by means of a traveling microscope. The air pressure served to cushion the mercury electrolyte system when it came to a

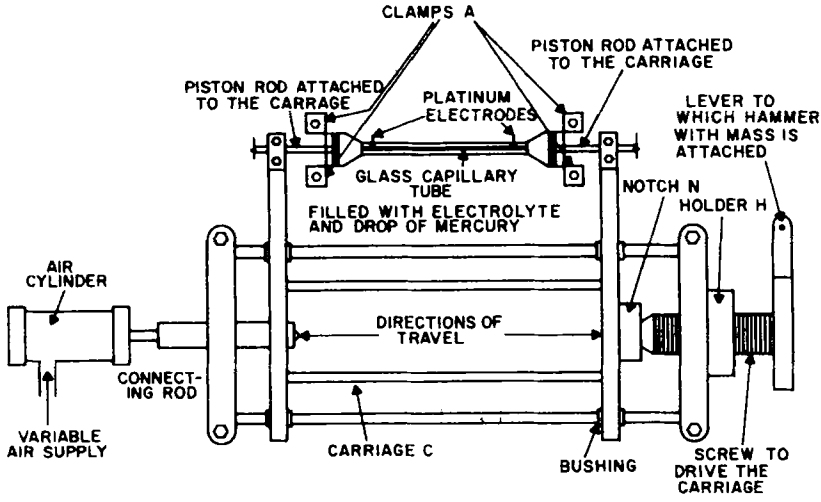

FIGURE 2 Top view of the apparatus for giving the mercury drop a constant acceleration.

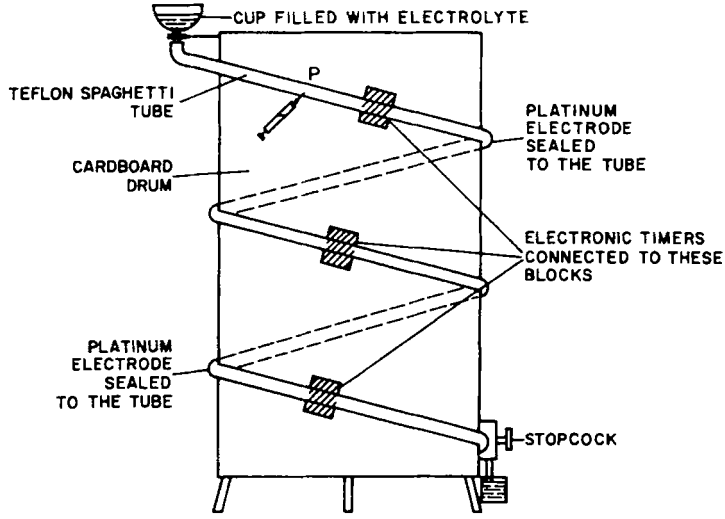

FIGURE 3 Apparatus for moving the mercury drop with constant velocity.

stop and thus prevented the mercury drop from breaking up. When the mercury drop moved relative to the tube an output voltage was measured across the two platinum leads, and was displayed on an oscilloscope.

A second experiment was designed in which the mercury electrolyte interfaces were made to move with a constant velocity. In order to do this, teflon tubes with internal diameters varying from 0.5 to 1.7 mm and about 2 meters long were wound around a cardboard drum as shown in Figure 3. The glass cup at the top and the tube were filled with electrolyte (1N $HClO_4$) and a single drop of mercury was injected into the tube at point P, by means of a syringe. When the stopcock was opened allowing the electrolyte to discharge at a constant rate, output voltages were measured across the platinum leads sealed into the tubes when the mercury drop was between the electrodes. The voltages were recorded on a strip chart recorder. By varying the rate of discharge and the length of the mercury drop, different output voltages were measured as long as the mercury drop moved between the platinum electrodes. The length of the mercury drop and the velocity with which it moved were measured by attaching electronic timers (photo cells) to the tube. Current measurements were made by directly connecting the platinum electrodes to a microammeter. The internal impedance of the tube was of the order of $10^4\ \Omega$ and that of the ammeter was of the order of $10\ \Omega$ and hence these are short circuit currents.

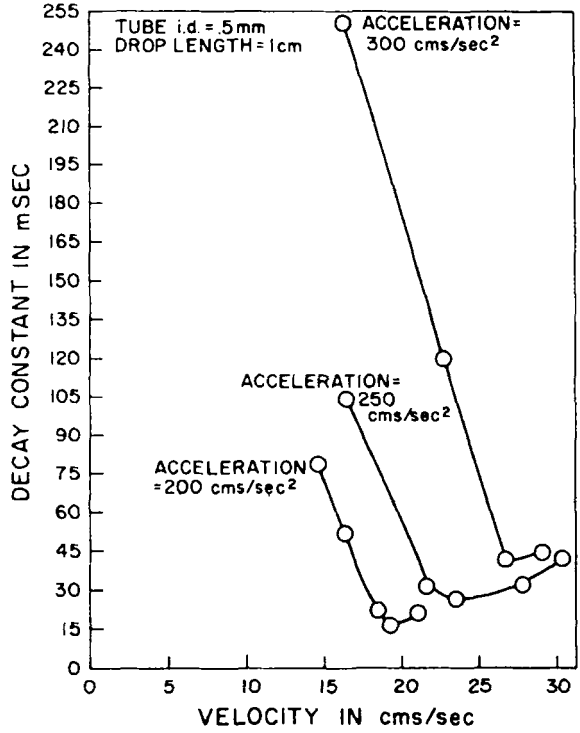

FIGURE 4 Dependence of the decay constant of a 1 cm drop on the velocity (for fixed acceleration).

III EXPERIMENTAL RESULTS

A Constant acceleration measurements

It was observed that as long as the drop in the tube moved relative to the tube, an output voltage was measured across the platinum probes. The output voltage increased as the acceleration increased up to a certain maximum velocity and then decayed exponentially when the drop came to an abrupt stop. The output voltage and decay were displayed on an oscilloscope and photographed. The exponential decays were fitted by means of least square to an equation of the form

$$V = V_0 e^{-t/\tau} \tag{1}$$

where V is the voltage. These decay constants, τ, are plotted as a function of the maximum velocity obtained for each mercury drop. Each drop was 1 cm long and three constant accelerations were used. These results are shown in Figure 4 and indicate that as the acceleration is increased the decay constant

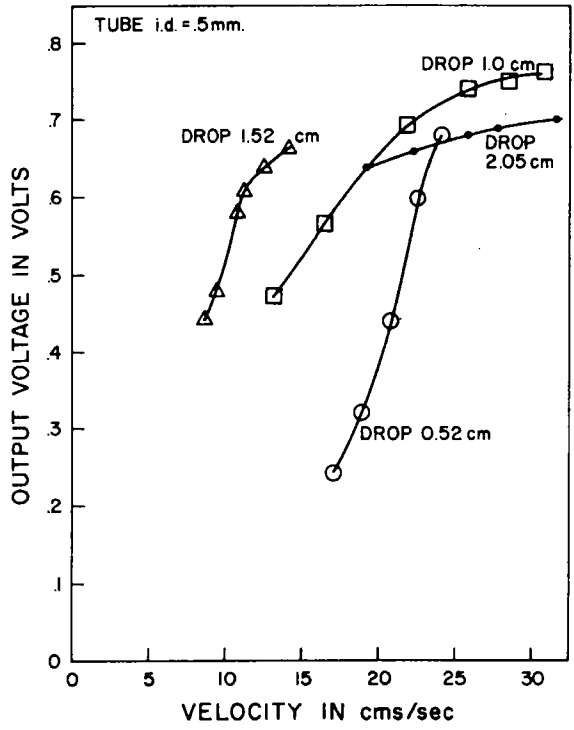

FIGURE 5a Dependence of the output voltage of different drop lengths on velocity for 0.5 mm i.d. tube.

increases. It should also be noted in Figure 4 that, as the maximum velocity increases the decay constant decreases and even indicates a minimum.

In Figures 5a and 5b, the maximum output voltages as determined from the photographs are plotted against the maximum velocities to which the drops were accelerated for different diameter tubes. The plot shows the output voltage to increase with the velocity and tends to saturate at high velocities. The output voltage was also found generally to increase with the length of the drop.

The dependence of the output voltages on velocity and acceleration of a drop 1.0 cm long were studied in 0.5 and 1 mm diameter tubes. The drop was given various constant accelerations for different lengths of time so that it would obtain different maximum velocities. The maximum output voltages were plotted against the maximum velocities of the mercury drops, these are shown in Figures 6a and 6b. These plots show that the output voltage increases with the velocity but decreases with increasing acceleration. This indicates that the velocity and acceleration have an opposite effect on producing the output voltage.

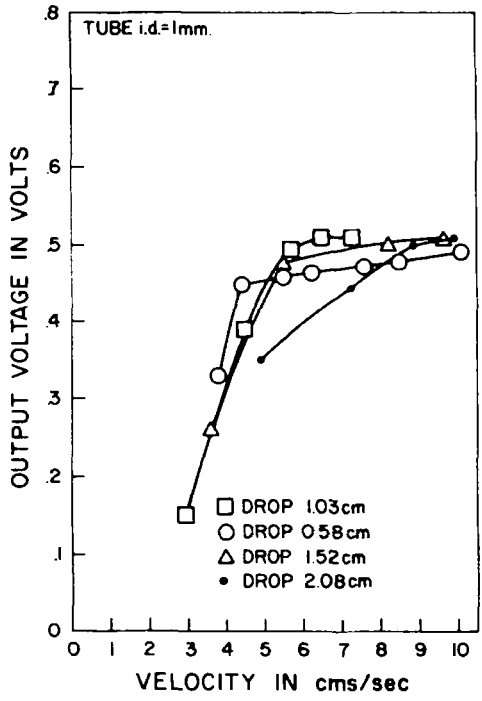

FIGURE 5b Dependence of the output voltage of different drop lengths on velocity for 1 mm i.d. tube.

B Constant velocity measurements

For a drop moving with constant velocity in the tube, an output voltage was also measured across the platinum electrodes. In this case, the output voltage was displayed on a strip chart recorder which had a large impedance ($5 \times 10^6\ \Omega$).

The output voltages were plotted against the drop lengths for different constant velocities, these plots are shown in Figures 7a and 7b. These plots show that the output voltage initially increases as the drop length increases and then saturates for very long drops. The output voltage also increases with the increase in the velocity of the drop, but no change was noted with change in the tube diameter. The polarity of the output voltage was positive in the direction of motion, which agrees with our previous experiment.

Current measurements were made by short circuiting the platinum electrodes with a microammeter. In Figure 8, the short circuit currents are plotted against the drop length for different velocities of the drops. The current is found to increase with an increase in the tube diameter.

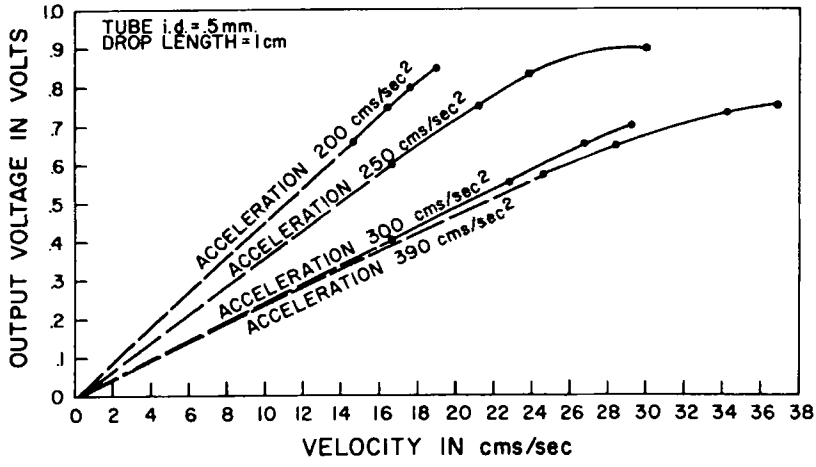

FIGURE 6a Dependence of the output voltage of a 1 cm drop length on the velocity for fixed accelerations in a 0.5 mm i.d. tube.

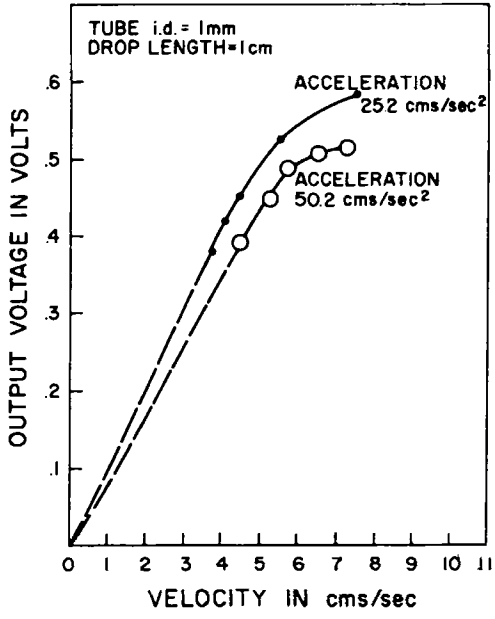

FIGURE 6b Dependence of the output voltage of a 1 cm drop length on the velocity for fixed accelerations in a 1 mm i.d. tube.

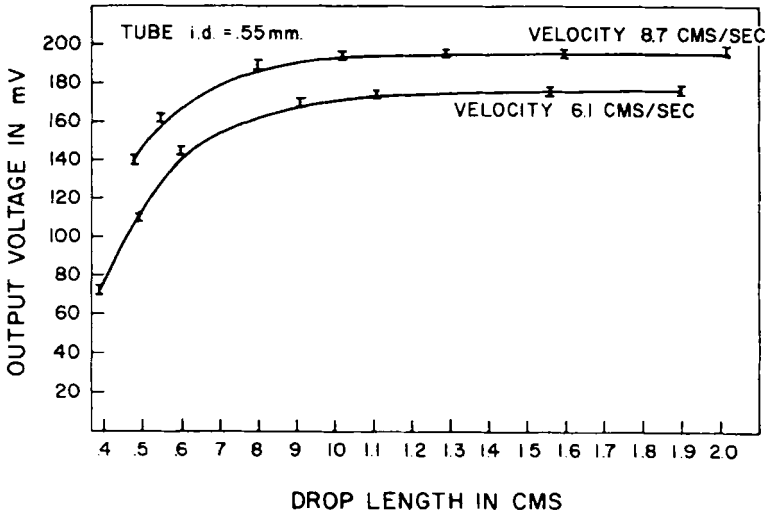

FIGURE 7a Dependence of the output voltage on the drop length for constant velocity motion for a 0.55 mm i.d. tube.

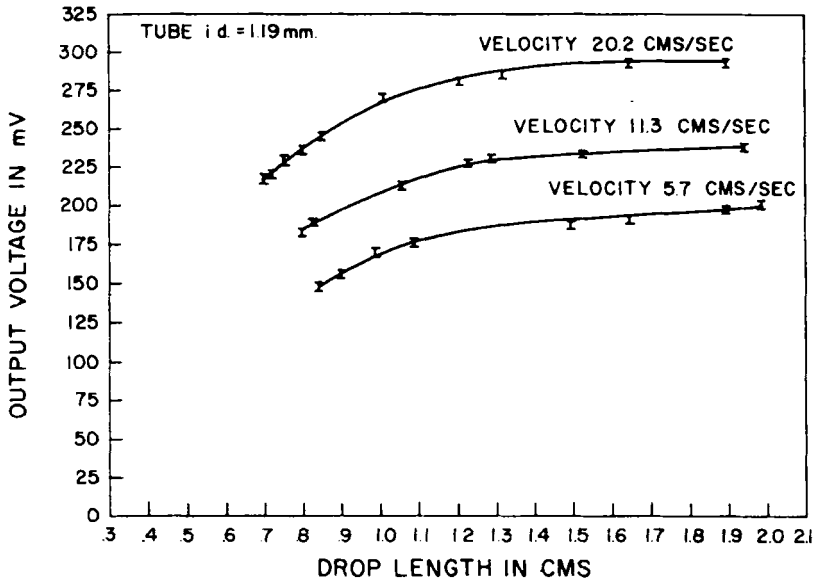

FIGURE 7b Dependence of the output voltage on the drop length for constant velocity motion for a 1.19 mm i.d. tube.

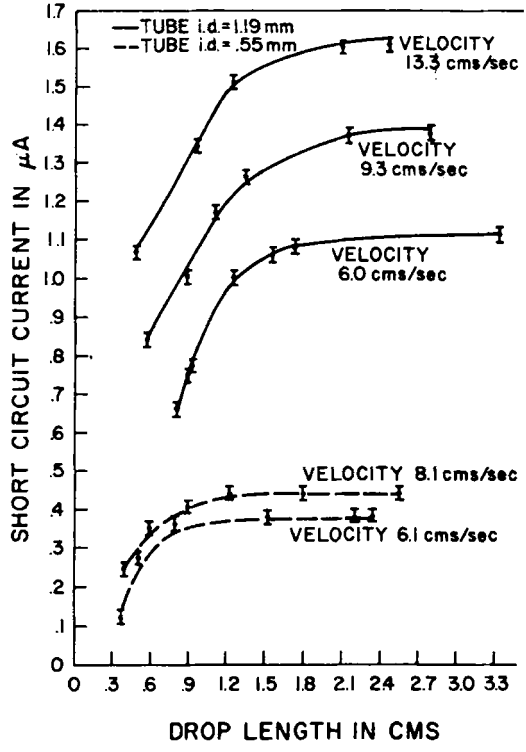

FIGURE 8 Dependence of the short circuit current on the drop length moving with constant velocity.

IV THEORY

In order to explain these experimental results we have devised a simple approximate theoretical treatment of the fluid dynamics of interfaces in a tube. The theory begins with the assumption that for a mercury-electrolyte interface in a capillary tube having a small enough internal diameter, the contact angle, θ which this interface makes with the capillary wall is determined by the radius of curvature of the interface which depends on the radius, a of the capillary tube.[8,9] Referring to Figure 9, it is seen that,

$$\cos\theta = \left.\frac{1}{\sqrt{1+\dot{r}^2}}\right|_{r=a}, \tag{2}$$

where in the axially symmetric cylindrical coordinate system shown, $[r(z), \theta, z]$, $\dot{r}$ is the derivative of r with respect to z, and we have chosen $r = a$

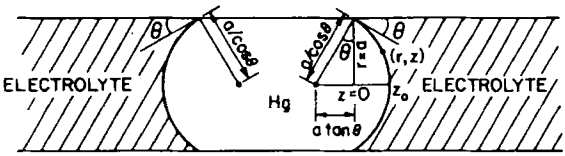

FIGURE 9 Figure 9 shows the dependence of the contact angle on the radius of curvature.

at $z = 0$. The pressure difference at any point across the interface is given by Rayleigh's formula,[6]

$$\Delta P_0 = P - P' = \gamma\left[\frac{1}{r\sqrt{\dot{r}^2 + 1}} - \frac{\ddot{r}}{(\dot{r}^2 + 1)^{3/2}}\right], \tag{3}$$

where P and P' are the pressures on the concave and convex sides of the interface respectively, and γ is the surface tension of the mercury surface in contact with the electrolyte and is measured in dynes/cm.

At $z = 0$, where $r = a$, then $\dot{r} = -\tan\theta$ and the equation of the surface can be integrated to give;

$$r(z) = \frac{a}{\cos\theta}\sqrt{1 - \left(\sin\theta + \frac{z\cos\theta}{a}\right)^2}. \tag{4}$$

The above equation shows that for a stationary mercury drop in a capillary tube and having electrolyte at both ends, the front as well as the back interface is a portion of a sphere with radius $a/\cos\theta$ and making a contact angle θ with the capillary tube. The surface area of each interface is,

$$A = \frac{2\pi a^2(1 - \sin\theta)}{\cos^2\theta}, \tag{5}$$

and the pressure difference across the interface in terms of the contact angle is

$$\Delta P_0 = \frac{2\gamma}{a}\cos\theta. \tag{6}$$

For the electrolyte-mercury-electrolyte system moving with constant velocity, the viscous forces of the fluid cause the pressure difference at the front and back ends of the mercury drop to be different from that of a stationary drop. The forces due to the viscosities of the fluids can be determined by considering an annular ring at the front end of the mercury drop which consists of the surface material of the interface and has a radius $r(z)$. The force on an annulus of the ring is,

$$F(r + dr) - F(r) = \frac{\partial F}{\partial r}\,dr, \tag{7}$$

where $F(r)$ is the force due to viscosities on a cylinder of radius r. Assuming laminar flow, $F(r)$ is,

$$F(r) = 2\pi r(\eta_e l_e + \eta_m l_m)\frac{\partial v_z}{\partial r}, \tag{8}$$

where η_e and η_m are the viscosities of the electrolyte and mercury respectively, l_e and l_m are the lengths of the electrolyte column and mercury drop respectively. The velocity, v_z is in the z direction and given by Poiseuille's equation,

$$v_z = v_0\left(1 - \frac{r^2}{a^2}\right), \tag{9}$$

where v_0 is the velocity at the center of the tube of radius a. If we now use Poiseuille's equation in Eq. (7), we get,

$$\frac{\partial F}{\partial r}\,dr = -8\pi(\eta_e l_e + \eta_m l_m)\frac{v_0}{a^2} r\dot{r}\,dz. \tag{10}$$

By assuming that the contribution to the force due to viscosity from the radial velocity v_r can be neglected as compared to the contribution from the axial velocity v_z, and also assuming that each interface behaves independently of the other, the pressure difference at any point on the front end of the moving drop is given by,

$$\Delta P_f = \Delta P_0 - 4\frac{(\eta_e l_e + \eta_m l_m)v_0}{a^2} = \gamma\left[\frac{1}{r(1+\dot{r}^2)^{1/2}} - \frac{\ddot{r}}{(1+\dot{r}^2)^{3/2}}\right], \tag{11}$$

and at the back end of the drop it is,

$$\Delta P_b = \Delta P_0 + 4\frac{(\eta_e l_e + \eta_m l_m)v_0}{a^2} = -\gamma\left[\frac{1}{r(1+\dot{r}^2)^{1/2}} - \frac{\ddot{r}}{(1+\dot{r}^2)^{3/2}}\right]. \tag{12}$$

The form of Eq. (11) and (12) is the same as Eq. (3) in that a constant (independent of z) appears on the left hand side. This means that the interfaces are the ends of a moving mercury drop which remain spherical in shape. If we now define for Eq. (3) an α_0 to be $\alpha_0 = \Delta P_0/\gamma$, then the corresponding $\alpha_\pm$ for Eqs. (11) and (12) is velocity dependent and is given by,

$$\alpha_\pm = \frac{1}{\gamma}\left[\Delta P_0 \mp \frac{4\bar{\eta}\bar{l}}{a^2} v_0\right], \tag{13}$$

where $\bar{\eta}\bar{l} = \eta_m l_m + \eta_e l_e$ and where the $\pm$ sign reflects the front or back respectively. Because of the small size of the capillary the value of $\alpha_\pm$ determines the contact angle and the area of the interfaces. The forces due to the viscosities of the fluids thus cause the two ends of the moving drop to

make different contact angles with the capillary walls and to have correspondingly different areas (cf. Eq. (5)). Substituting Eq. (5) into Eqs. (11) and (12) yields a contact angle at the front end of,

$$\cos \theta_{fv} = \cos \theta - \frac{2\eta \bar{l} v_0}{\gamma a}, \tag{14}$$

and a contact angle at the back of,

$$\cos \theta_{bv} = \cos \theta + \frac{2\eta \bar{l} v_0}{\gamma a}. \tag{15}$$

Thus for a mercury drop moving with constant velocity, the front interface tends to flatten and the back interface tends to become more nearly hemispherical. At some velocity, v_{0x} the back interface becomes a hemisphere ($\theta_{b(v_{0x})} = 0$) and for velocities greater than v_{0x} it cannot bulge out any further since this would violate the requirement in Eq. (12) that the interface remains spherical in shape. However, for velocities greater than v_{0x}, the front interface can keep flattening until its minimum area would approach that of a circular disk. Thus, v_{0x} is the velocity at which one would expect a change over from the behavior which reflects both ends of the mercury drop deforming ($v_0 < v_{0x}$) to only one end deforming ($v_0 > v_{0x}$).

If in Eq. 14, we apply the condition that when $\theta_{bv} = 0$, $v_0 \equiv v_{0x} \equiv 2v_x$, this gives,

$$v_x = \frac{v_{0x}}{2} = \frac{\gamma a}{4\eta \bar{l}}(1 - \cos \theta), \tag{16}$$

where v_x is the experimentally determined velocity of the whole mercury slug. For Poiseuille flow the velocity v_x is one half of v_0 (the z component of the Poiseuille velocity at the center of the drop) the parameter v_x is the characteristic velocity at which the velocity dependence of the potential changes for a drop. Knowing v_x for a particular drop allows us to estimate the contact angle θ for a stationary drop.

We assume the output voltage, E across a moving drop is due to the difference in the dipole moment density at each end of the mercury drop because of the distortion of the surface areas at the ends (for a detailed analysis of the formation of the double layer see Bockris and Reddy[10]). Implicit in this assumption is the hypothesis that the total number of dipoles across the double layer does not change when the ends are deformed. From these assumptions the output voltage across the moving drop can be shown to be

$$E = \frac{\mu}{\kappa \varepsilon_0}\left(\frac{1}{A_f} - \frac{1}{A_b}\right), \tag{17}$$

where μ is the dipole moment across the interface, κ is some average dielectric constant between the dipole layer, ε_0 is the permittivity of free space, A_f and A_b are the surface areas of the front and back of the moving drop respectively. The maximum output voltage, E_{max}, will occur when the back end of the moving drop becomes a hemisphere and the front end becomes a circular disk, we can write the above equation as,

$$E = E_{max}\left(\frac{2\pi a^2}{A_f} - \frac{2\pi a^2}{A_b}\right), \tag{18}$$

where $E_{max} = \mu/\kappa\varepsilon_0 2\pi a^2$, and would be the potential across a single interface. Thus, for a drop moving with constant velocity the output voltage across the drop is,

$$E_r = E_{max}\left(\frac{2\pi a^2}{A_{fv}} - \frac{2\pi a^2}{A_{bv}}\right). \tag{19}$$

The surface areas of the front and back ends of the drop are found from Eq. 5 to be,

$$A_{fv} = 2\pi a^2 \frac{(1 - \sin\theta_{fv})}{\cos^2\theta_{fv}}, \tag{20}$$

and

$$A_{bv} = 2\pi a^2 \frac{(1 - \sin\theta_{bv})}{\cos^2\theta_{bv}}. \tag{21}$$

These equations should adequately describe the constant velocity experiment.

To describe the deformation of the interfaces in a dynamical situation involving non-zero acceleration of the drop, requires the solution of the equivalent of Navier–Stokes equation for the interfaces. However, for a mercury drop moving with constant acceleration a phenomenological approach can be used to obtain the surface areas of the front and the back ends of the moving drop. We utilize the analogy that a constant acceleration is like gravity and infer the pressure change in the tube due to this acceleration. Rivers[11] has shown that when a capillary tube containing a mercury drop having electrolyte at both ends is acted on by a small force for a short time such that this force does not cause any relative motion between the drop and the capillary wall, the effect of this force is to distort the surface areas of the front and the back ends of the drop. Using perturbation theory he has found the surface area of the back end, S' to be,

$$S' = S\left[1 + \tfrac{1}{6}a^2\left(\frac{\rho_m - \rho_e}{\gamma}\right)A\right], \tag{22}$$

where S is the surface area of the stationary (unperturbed drop), a is the radius of the capillary tube, ρ_m and ρ_e are the densities of mercury and electrolytes respectively, γ is the surface tension of the mercury surface in contract with the electrolyte and A is the acceleration given to the capillary tube.

We incorporate this approach into our constant velocity results by introducing and adjusting a parameter C in place of the $\frac{1}{6}$ and use these expressions to determine the surface area of a drop moving with constant acceleration by assuming that the force causing the acceleration also causes a small perturbation to the surface areas of the drop moving with constant velocity (zero acceleration). This gives for the area of the front surface,

$$A_{fA} = A_{fv'}\left[1 + Ca^2\left(\frac{\rho_m - \rho_e}{\gamma}\right)A\right], \tag{23}$$

and the area for the back surface is,

$$A_{bv} = A_{bv'}\left[1 - Ca^2\left(\frac{\rho_m - \rho_e}{\gamma}\right)A\right], \tag{24}$$

where C is our adjustable parameter, A is the acceleration given to the drop and $A_{fv'}$, and $A_{bv'}$ are the surface areas of the front and back ends for a drop moving constant velocity. The output voltage across a drop moving with constant acceleration is obtained by replacing A_f and A_b in Eq. 18 by A_{fA} and A_{bA}. The output velocity is then given by,

$$E_A = E_{\max}\left[\frac{2\pi a^2}{A_{fv'}\left[1 + Ca^2\left(\frac{\rho_m - \rho_e}{\gamma}\right)A\right]} - \frac{2\pi a^2}{A_{bv'}\left[1 - Ca^2\left(\frac{\rho_m - \rho_e}{\gamma}\right)A\right]}\right]. \tag{25}$$

For finite acceleration and zero relative velocity, the above equation gives small output voltages (U-effect II) as compared to the output voltage for a drop moving with constant acceleration and having a finite velocity with respect to the capillary tube (U-effect III). The dependence of the output voltage on acceleration is opposite to that of velocity and hence U-effect II has an opposite polarity to that of U-effect III.[6]

V ANALYSIS

As shown by Eq. (25), the output voltage, E was found to be a function of the acceleration, a, of the mercury drop, the velocity, v, with which the drop moved, the length, l, of the drop, and the radius, r, of the capillary tube, i.e.,

$$E = f(a, v, l, r). \tag{26}$$

The force due to the viscosity acting on a moving drop is proportional to v/r and for low velocities the output voltage, E should be proportional to the force, F, the product Er should be linearly dependent on the velocity of the drop. For a 1 cm drop, the plots of the output voltage versus velocity as shown in Figures 6a and 6b were transferred onto a single plot by reducing the velocity and acceleration of this drop in two different diameter tubes by use of the continuity equation,

$$A_{0.5}X_{0.5} = A_1X_1 \tag{27}$$

where $A_{0.5}$ and A_1 are the cross-sectional areas of the 0.5 and 1 mm diameter tubes and $X_{0.5}$ and X_1 is the velocity or acceleration in these two tubes depending on which is being transformed.

The product of the output voltage, Er and the radius of the tube in which it was obtained versus the reduced velocity (reduced to 1 mm diameter tubes) of the drop are shown in Figure 10. In these plots, the points for the "same" acceleration fell on one curve. The curves were extrapolated to the origin, since for zero velocity the output voltage (due to U-effect II) is quite small (0.05 volts).[3,4] Each curve shows a change of slope at some velocity v_t. This

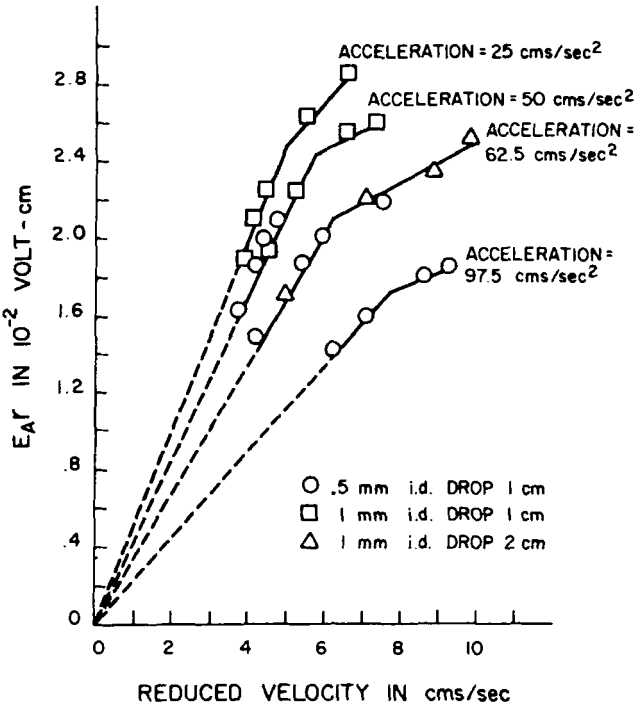

FIGURE 10 Dependence of E_Ar on reduced velocity.

TABLE I

Computed values of E_{max} and C for drop having different constant accelerations

Acceleration cm/sec^2	E_{max} volt	C
25	0.7221	6.318
50	0.7059	5.320
67.5	0.6008	4.016
97.5	0.4820	3.394

is consistent with the theory in which we considered the interfaces to always be some portion of a sphere and at the velocity v_t, the back interface becomes a hemisphere and can make no further contribution to the net change in area of the two interfaces. For velocities greater than v_t, the slope is less than for velocities less than v_t. Again, this fits in with our theory since only the front interface can continue to deform for velocities greater than v_t. When the velocities, v_t were plotted against the respective accelerations (Figure 10) a straight line was obtained which had an intercept (velocity for zero acceleration) of 4.4 cms/sec on the velocity axis. This value of the velocity, denoted by v_x, was used in Eq. 16 to determine the contact angle θ. For typical values of $\gamma = 375$ dynes/cm, $a = 0.05$ cm, $\eta_e = 1$ c.p., $\eta_m = 1.5$ c.p., $l_n = 1$ cm and $l_e = 12$ cm, θ was determined to be 29°.

The value of $\theta = 29°$, and the values of E_A, v, and v_t from Figure 10, were used in Eq. 25 to calculate the parameters E_{max} and C. Table I shows the values of E_{max} and C as a function of acceleration. The parameter E_{max} should be independent of acceleration and essentially is for acceleration less than 50 cm/sec^2. The variation of E_{max} for larger accelerations shows the limitations of our simple interpolation Eqs. (23) and (24).

A plot of the output voltage E_A versus v/v_t for different accelerations obtained by using Eq. (25) are shown in Figure 11. The agreement between experiment and theory can be seen by comparing Figures 10 and 11. The experimental and theoretical plots have the same general shape.

For a drop 1 cm long moving with constant velocity, the product $E_v r$ versus reduced velocity (all for a 1 mm diameter tube) is shown in Figure 12. Using the value of v_x (4.4 cms/sec), the surface areas of the front and back end of drops moving with constant velocity were calculated. These values were used in Eq. (19) to find E_{max} which would make the theoretical curve fit the experimental curve in Figure 12. The value of E_{max} obtained by this procedure was 0.35V. It is possible that gravity distorted the surfaces in the constant velocity experiment and this could have resulted in a value of E_{max} smaller than given in the horizontal tubes.

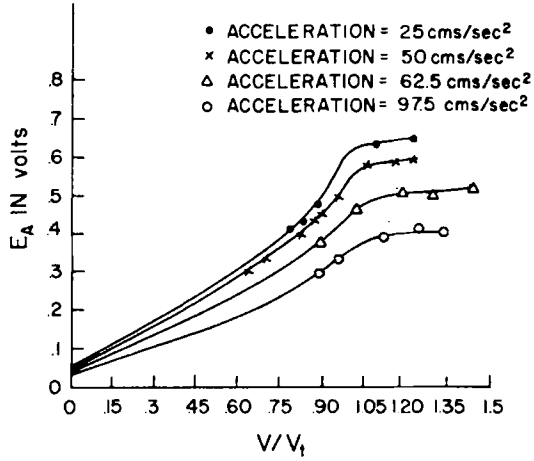

FIGURE 11 Theoretical plots of E_A versus v/v_i.

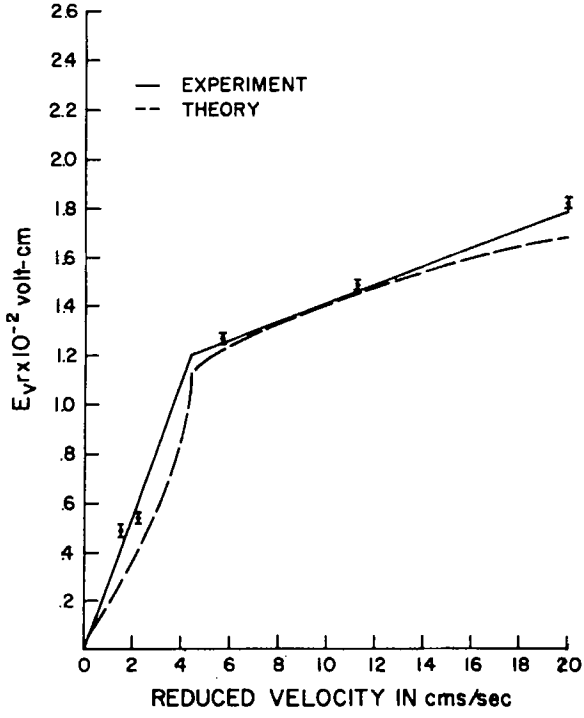

FIGURE 12 Plot of $E_v r$ versus reduced velocity.

VI CONCLUSION

These experimental results and the simple theory which has been used to interpret them are the first work which suggests that the U-effect II and U-effect III are manifestations of the deformations of the surface areas of the mercury slug. These results allow a first step in the process of determining a microscopic understanding of these electromechanical effects in systems with polarizable and deformable interfaces.

The major result of this work may be the indication that by combining mechanical perturbations to the interface and deriving from such experiments the theoretical parameter E_{max}, an independent determination of the potential across the mercury-acid interface at zero external potential will have been made. This may prove to be useful in electrochemical applications.

While the theory and experiment presented here provide a coherent picture of this phenomena, several interesting extensions of these results need to be examined in order to establish whether a new area of interaction between the physicist and the electrochemist will have been opened up.

Acknowledgment

The authors would like to thank Mr. Robert W. Ross for designing and constructing much of the equipment used in the experiment.

References

1. V. G. Levich, *Physicochemical Hydrodynamics*, Prentice-Hall Inc., Englewood Cliffs, N.J., 1962.
2. Edgar Newbery, *Transactions of the Electrochemical Society*, **69**, 611, 1936.
3. S. Ueda, A. Watanabe, and F. Tsuji, *J. Electrochem. Soc. Japan*, **19**, 142 and 153, 1951; *J. Electrochem. Soc. Japan*, **20**, 605, 1952; *J. Electrochem. Soc. Japan*, **21**, 14, 1953.
4. S. Ueda, F. Tsuji, and A. Watanabe, *Int. Cong. of Surf. Activity, Proc. 2nd, London*, **3**, 3, 1957.
5. W. Fain, S. Brown, and A. Lockenwitz, *J. Acous. Soc. Amer.* **29**, 902, 1957.
6. B. Podolsky, G. Kuskevics, and J. Rivers, *J. Applied Physics*, **28**, 357, 1957.
7. B. Christiansen, *Ann. Phys., Ser. 4*, **12**, 1072, 1903.
8. R. Payne, *J. Electroanalysis. Chem.*, **7**, 343, 1964.
9. L. D. Landau, and E. M. Lifshitz, *Fluid Mechanics*, Pergamon Press, 1959.
10. T. Bockris, O'M., and A. K. Reddy, *Modern Electrochemistry*, Plenum Press, N.Y., Volume 2, Ch. 7, 1970.
11. J. L. Rivers, Ph.D. Thesis, Univ. of Cincinnati, 1956.